A complete framework for personalised modeling and control of children's cerebral palsy

Sabrina Otmani, Guilhem Michon, Bruno Watier

A complete framework for personalised modeling and control of children's cerebral palsy

Sabrina OTMANI[1,2], Guilhem MICHON[1], Bruno WATIER[2]

***Abstract*— Two 9 years old twin sisters, one with spastic cerebral palsy (C) and the other healthy (H) without any impairments, performed the pendulum drop test with EMG acquisitions. The purpose of this paper is to present a way to model the knee's spastic angular displacement of C and H using mechanical differential equations. Then, we propose a controller to correct the knee's angular displacement of C. and make it converge towards the one of H. To this end, we use a PID controller to correct the angular position. Both models of the spasticity and the controller were computed using a genetic algorithm (GA). Angular trajectories were modeled with a determination coefficient (R^2) higher than 95% for both spastic and non-spastic cases, and R^2 > 87% for the corrected angular position of C.**

I. INTRODUCTION

This paper is part of a project to create a customized exoskeleton for the child with a specific spastic cerebral palsy and with the final purpose to determine how it can correct or enhance the gait of this child.

Cerebral palsy (CP) is a "group of non-progressive, but often changing, motor impairment syndromes secondary to lesions or anomalies of the brain arising in the early stages of development" [1]. It is the most common cause of motor disability during childhood in developed countries, with an incidence of 2.0 to 2.5 per 1000 live births. Different causes can provoke CP as gene abnormalities, malformations, cerebral hypoxia or prematurity. The severity of the CP is quantified using Growth Motor Function Classification System (GMFCS): it is decomposed into 5 levels from the lowest severity to the highest. CP also has subtypes like ataxic CP, dyskinetic CP and spastic CP which is the subject of this paper. It is also reported in [2] and [3] that spasticity is the most common disabling condition seen in cerebral palsy. Spasticity is a condition in which there is an abnormal increase in muscle tone or stiffness of muscle, which might interfere with movements, gait and speech while causing discomfort or pain. It creates pathological and involuntary reflexes [4], [5]. Spasticity is known to be a "hypersensitive, velocity-dependent response to passive muscle stretch" and also position-dependent [6],[7],[8]: the quicker the movement is, the higher is the effect of the spasticity. It is a symptomatic behavior of involuntary muscle activations due to the hypersensitivity of stretch reflex loops. It is then both dependent on joints position and joints velocity. Exoskeletons are nowadays widely used to improve the walking of people with cerebral palsy, especially spastic ones. Rehabilitation is a key to enhancing motor impairment but "management of spasticity should be multimodal" [9] and can be combined with medication such as botulinum toxin. The pendulum drop test is a way to characterize spasticity. It was first developed by [10] then by [11] and [12]. This method was used in [6] to compute the knee angular trajectory of 3 brothers, two of them with cerebral palsy.

In this paper, we first focus on the modeling of the effect of the spasticity on a pendulum knee drop test of a 9 years old girl called C. who has CP with a GMFCS level of 2. Then, we propose to control the angular trajectory of the knee joint, using a PID controller.

II. RELATED WORK

1) Spasticity model: Different methods have been developed to design a spasticity model as [6], [13], [14]. [6] focuses their work on the muscular contribution in the knee angular displacement during a pendulum drop test to clearly put forward the active process of the knee rotation of subjects with spasticity. Considering the traditional terms in the mechanical equation such as inertia and gravity, [6] defined additional velocity-feedback torques to highlight the velocity-dependent aspect of spasticity. The activation period of this torque during the pendulum cycle and its amplitude were defined using an optimization algorithm without any consideration for muscular activity. This specification can enhance the performance of the fitting model. However, this model could be a source of inaccuracy when it conceals the actual origin of spasticity, which is an involuntary and pathological activation of the muscles [4][5]. In this context, the first main contribution of our work to this issue is first, the realisation of pendulum drop tests on twin sisters with EMG acquisitions. Then, the second main contribution of our work to this issue is to specify the activation period of these torques by using onsets and offsets of muscular activations extracted from EMG data. We also design additional position-feedback torques to bring forward the position-dependent character of spasticity with the same timing as velocity-feedback torques [8]. The amplitude of those torques was defined using GA.

2) Control of spasticity: PID schemes are widely used in the literature as an efficient method to control exoskeletons [15] and also human gaits in exoskeletons [16], [17]. In [16], the purpose is to correct the crouch gait of subjects with cerebral palsy. It corresponds to our goal and is an interesting starting point for our control. Position control is one of the most used methods to correct errors between the reference

[1]Université de Toulouse, CNRS, ICA, ISAE-SUPAERO, Toulouse, France

[2]LAAS-CNRS, Université de Toulouse, CNRS, UPS, France

and the measured value. PID gains are then essential to determine. Different methods are used: manually as in [16], using the Ziegler-Nichols method [18] or also using GA as in [17]. The main contribution of this paper is the use of GA as a technique to find the optimal parameters for the proposed PID controller.

3) Human-exoskeleton coupling: The interface between the human and exoskeleton can be modeled as 2 systems in parallel with a rigid constraint which implies the same output for both systems [19][20]. In [19], local deformations of the skin and muscles due to the exoskeleton's strap are not considered and can be specified accurately and completely as in [20]. In this context, the main outcome of this work is to design a simple model of a human-exoskeleton interface based on a damped spring torque [21]. Stiffness and damping coefficients were identified using GA.

III. Modeling of the Spasticity Using a Genetic Algorithm (GA)

A. Methods

The modeling of the knee-muscle spasticity is performed using equations developed in [6]. An additional position-dependent term was added to underline the dependent nature of spasticity. An experiment, based on the EduExo (Robotic Exoskeleton Kit) is used to obtain the kinematic and EMG data. The system is composed of thigh and calf supports 3D printed interfaces integrating angle sensors as presented in Figure 1. Two ElectroMyoGrams (EMG) sensors (MyoWare from SparkFun) are added to study muscle activity. EMG probes are located on two precise muscles (medial gastrocnemius and vastus lateralis) based on the SENIAM recommendations [22] which are agonist and antagonist muscles for the knee joint. The knee's angular positions and EMG signals are measured at a sampling frequency of 70Hz imposed by the system and the data collected [6].

Two 9 years old twin sisters, one with spastic cerebral palsy (C) and the other healthy (H) without any impairments, performed a pendulum drop test. Before data collection, we obtained informed consent and assent from the parents and the twin, respectively. The parents also have signed an informed agreement that the Declaration of Helsinki is respected during the experiment. This test aims to determine the knee's angular displacement. Each child sat on a seat, which allowed the lower shanks of the legs to swing freely about the knee. Then, the experimenter moved passively the leg in rotation until a certain desired angle which will correspond to the initial position condition. The children were asked to not actively participate in the movement during the acquisition. These pendulum drop tests are used to characterize the rheological model of a spastic knee by studying the pendular movement of the knee due to gravity. Two types of drop test acquisition are recorded, in extension (e) and in flexion (f) with the given initial conditions: $\Theta_0 \approx \pm 25°$ ($\Theta_0 = 0°$ being the vertical position) and $\Theta'_0 = 0°.s^{-1}$. Those drops were performed for each leg of each twin 10 times.

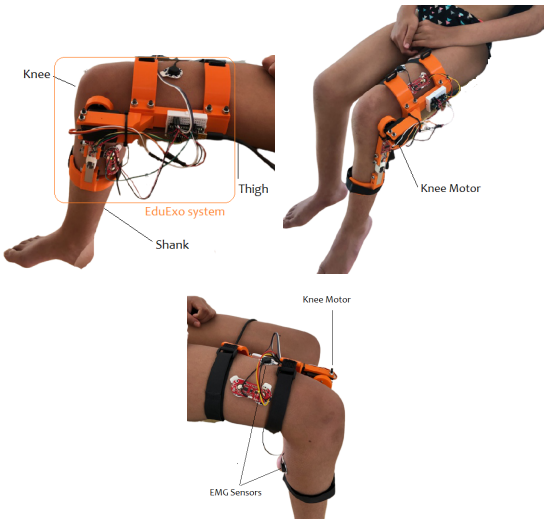

Fig. 1. Overview of EduExo hardware on a child's leg.

The mean difference between the two anthropometries is around 11.2% (see column "gap" in Table I). The masses of the segments were computed using regression equations of [23] for children of 9 years old. For the modeling, the twins are considered to have the same anthropometry, the one of C.

TABLE I
ANTHROPOMETRY OF THE TWO TWINS

Parameter	H.	C.	Gap (%)
Height (cm)	134	123	8.2
Body weight (kg)	25	22	12
Length of the shank (cm)	32	28	12.5
Mass of the shank (kg)	1.25	1.1	12
Mass of the foot (kg)	0.52	0.46	11.5

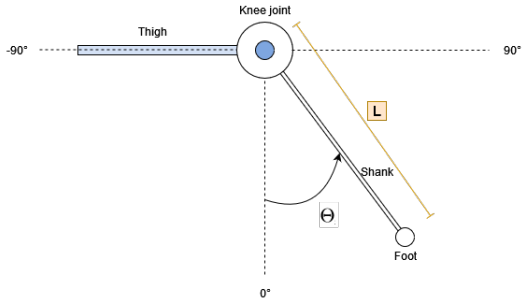

Fig. 2. Schematic view of the leg.

Once the data are collected, the knee trajectories were modeled using the equations defined in [6] and additional position-dependent torques. The schematic view of the leg is presented in Figure 2. The foot is considered as a point mass at the end of the shank. The equation of motion of the knee angle Θ is given by the following differential equation for

extensors (subscript e, when $\Theta' < 0$) and flexors (subscript f, when $\Theta' \geq 0$) :

$$I\Theta'' + B_{e,f}\Theta' + K_{e,f}\Theta + T_{e,f} + B\Theta' + K\Theta = mgLsin(\Theta) \quad (1)$$

with :

- Θ, Θ', Θ'': joint angle, velocity and acceleration.
- I: moment of inertia of the shank and the foot expressed at the center of the joint,
- B_e, B_f: damping coefficients,
- K_e, K_f: stiffness coefficients,
- T_e, T_f: nonlinear stiffness torques defined by [24] as $K1_{e,f}(e^{-K2_{e,f}\Theta} - 1)$
- m: mass of the shank and the foot,
- g: gravity acceleration,
- L: distance from the joint to the shank's center of mass + the distance between the joint and the foot center of mass,
- $B = B_E$ or B_F : velocity feedback gains for extension (B_E) or flexion (B_F).
- $K = K_E$ or K_F : position feedback gains for extension (K_E) or flexion (K_F).

B_E and B_F gains are applied at a given time (the onsets) and during a certain duration (the delays). Those gains multiplied by the joint speed are used to model the contribution of the velocity in the spasticity. K_E and K_F gains are applied at the same time as B_E and B_F and are the novelty of this model. Those gains multiplied by the joint position are used to model the limit of the angular position due to the spasticity. The spastic torques are velocity and position-dependent [6],[7]. However, the relationship between these torques and muscular activity remains an open problem. In this paper, we assume the onsets and the delays as values corresponding to the beginning and the duration of the muscular activity of the extensor and flexor muscles.
The values of the damping coefficients (B_e and B_f), spring coefficients (K_e and K_f), and K1/K2 from the non-linear stiffness torques remain unknown and will be determined using a GA. This method is used to solve constrained but also unconstrained optimization problems based on a natural selection process that copies biological evolution [25] (Figure 3). It is easy to implement and to interate on it. It allows the determination of the model parameters by minimizing a cost function.

A chromosome is a vector of parameters determined by the GA to minimize this cost function. Thus, in this paper, the chromosome (Chr) for the model of the knee trajectory is described as follows:

$$\begin{aligned} Chr = [&Ke, Kf, B_e, B_f, K1_e, K2_e, K1_f, K2_f, \\ &B_F(1), B_F(2), B_F(3), B_E(1), B_E(2), B_E(3), \\ &K_F(1), K_F(2), K_F(3), K_E(1), K_E(2), K_E(3)], \end{aligned} \quad (2)$$

To summarize, B_F, B_E, K_F and K_E are in Chr defined as vectors of three values representing the gains of the velocity and position feedback torques for each muscular activation during the acquisition. The velocity and position

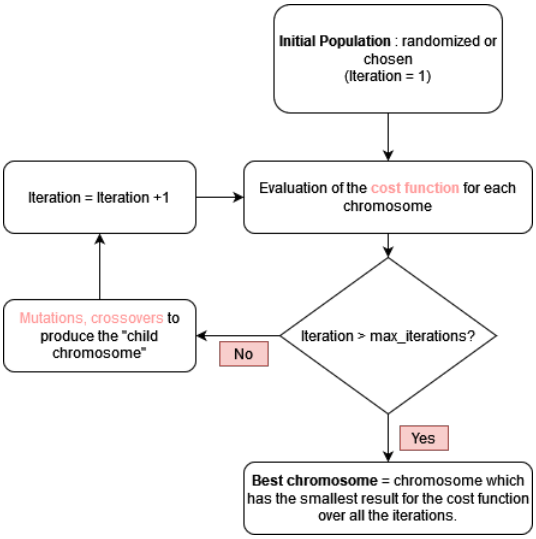

Fig. 3. Flowchart of genetic algorithm (GA).

gains of the feedback torques are still unknown and will be determined later in the paper.
H represents the case of the non-pathology, without spasticity so for this model, B_F, B_E, K_F and K_E are set to zero. To determine the values of the chromosome Chr, the genetic algorithm was computed with the following parameters:

- Number of parameters: 8 for H's model and 20 for C.'s model.
- Number of iterations: 5000,
- Number of chromosomes to test at each iteration: 300 chosen randomly by the GA,
- Maximum stall generation: 500,
- Function tolerance value: $1e^{-5}$.

The function tolerance value represents the minimal value considered to determine if 2 consecutive optimal chromosomes have a real different cost function. The cost function used (Equation 3) is based on the error of the model angular positions (determined by the resolution of the differential equation using ODE45 with a time step of $0.001s$) and the experimental angular positions of the knee. The cost function used is based on the coefficient of determination (R^2). The cost function is defined as follows :

$$Cost\_Function = 1 - R^2 = \frac{\sum_{i=1}^{m}(y_i - \hat{y_i})^2}{\sum_{i=1}^{m}(y_i - \bar{y})^2} \quad (3)$$

with :

- m: number of experimental measurements,
- y_i: value of the measurement i,
- $\hat{y_i}$: corresponding simulated data,
- $\bar{y}$: mean of all the measurements.

Data processing:

a) Angular displacement values: Knee's angular displacement values of H. and C. were filtered using a lowpass filter with a cutoff frequency of $6Hz$ [16].

b) EMG: EMG signals are full-wave rectified and were filtered using a lowpass filter with a cutoff frequency of $8Hz$ [26].

Two pendulum drop tests are presented for each twin H and C:
- One with the beginning of flexion (Pendulum 2 for H and Pendulum 2 for C).
- One with the beginning of extension (Pendulum 1 for H and Pendulum 1 for C).

B. Results

TABLE II

VALUES OF 20 PARAMETERS COMPOSING THE FINAL CHROMOSOME FOR THE PENDULUMS 1 AND 2 OF C.

Pendulum 1	Ke	Kf	Be	Bf	$K1_e$	$K2_e$	$K1_f$
	2.98	2.52	1.1614	0.4377	1.85	0.49	1.24
	$K2_f$	$B_F(1)$	$B_F(2)$	$B_F(3)$	$B_E(1)$	$B_E(2)$	$B_E(3)$
	0.72	0.05	9.36e-4	0.09	0.008	0.07	0.01
	$K_F(1)$	$K_F(2)$	$K_F(3)$	$K_E(1)$	$K_E(2)$	$K_E(3)$	
	0.002	0.48	-0.2	0.1	-0.48	0.05	
Pendulum 2	Ke	Kf	Be	Bf	$K1_e$	$K2_e$	$K1_f$
	3.44	2.35	0.08	0.06	1.62	1.49	1.83
	$K2_f$	$B_F(1)$	$B_F(2)$	$B_F(3)$	$B_E(1)$	$B_E(2)$	$B_E(3)$
	1.16	0.17	0.05	0.01	0.06	0.11	0.37
	$K_F(1)$	$K_F(2)$	$K_F(3)$	$K_E(1)$	$K_E(2)$	$K_E(3)$	
	0.2	0.18	0.1	0.27	0.19	0.1	

TABLE III

VALUES OF 8 PARAMETERS COMPOSING THE FINAL CHROMOSOME FOR PENDULUMS 1 AND 2 OF H.

Pendulum 1	Ke	Kf	Be	Bf	$K1_e$	$K2_e$	$K1_f$	$K2_f$
	1.74	0.20	0.04	0.05	0.48	1.99	0.66	1.45
Pendulum 2	Ke	Kf	Be	Bf	$K1_e$	$K2_e$	$K1_f$	$K2_f$
	1.40	$1e^{-5}$	0.060	0.11	0.73	1.81	0.69	0.61

For H: H. represents the case of the non-pathology, without spasticity. A normal drop test does not create or provoke any muscular activations, only gravity affects the leg. It is admitted [6] that in the case of a healthy child, H. does not have any muscular activations and does not have any velocity/position-dependent torque to model the leg behavior.

For C:

The orange and pink signals in Figure 4 represent the period when an activation starts and ends for the pendulum 2 of C. It is presented as a Heaviside function for better comprehension and to see easily the link between the activations and the knee's angular displacement.

Three muscular activations per pendulum drop test (for the flexor muscle and the extensor muscle) were recorded and studied as in [6]. Values are reported in Table IV.

Some activations were not clear due to the difficulties during the acquisitions (pathological child, sensor placements, the effect of the fatigue during the acquisitions) and were not considered.

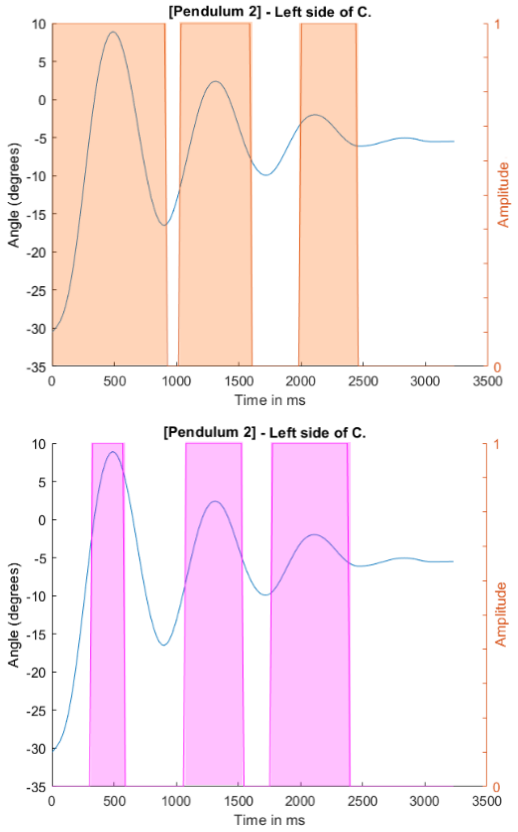

Fig. 4. Knee's angular displacement (blue) and muscular activity of the flexor muscle (bottom, pink) and extensor muscle for pendulum 2 (top, orange) represented as a Heaviside function.

TABLE IV

VALUES OF THE ONSETS (MS) AND DURATION (MS) OF THE ACTIVATIONS OF THE PENDULUM 1 AND 2 OF C.

	Flexor		**Extensor**	
Pendulum 1	Onset (ms)	Duration (ms)	Onset (ms)	Duration (ms)
1st activation	60	600	159	559
2nd activation	680	300	736	323
3rd activation	1427	443	1059	599
Pendulum 2	Onset (ms)	Duration (ms)	Onset (ms)	Duration (ms)
1st activation	323	267	0	907
2nd activation	1078	465	1015	590
3rd activation	1772	623	2002	436

1) Pendulum modeling:

a) For H: The velocity and position feedback, which have the goal to mimic the contributions of the spasticity on the knee movement, are set to zero ($B_E = B_F = K_E = K_F = 0$) as long as H is not pathological.

The simulated and measured knee's angular displacements of H. are presented in Figure 5. These results highlight the same amplitudes and frequencies between the simulated and measured data and are obtained with $R^2 = 96.7\%$ for pendulum 1 (mean error: $0.37° \pm 1.4°$) and $R^2 = 97.4\%$ for pendulum 2 (mean error: $0.63° \pm 1.02°$).

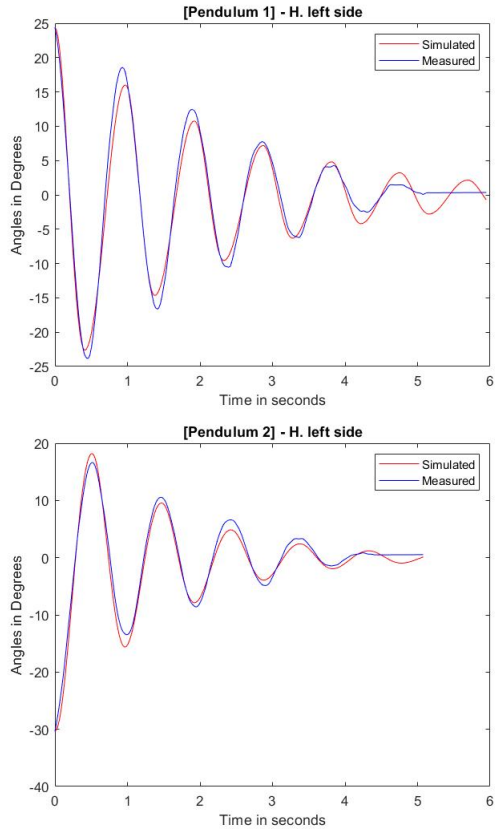

Fig. 5. Experimental **(measured)** and modeled **(simulated)** knee trajectory for the initial condition in extension (pendulum 1) and flexion (pendulum 2).

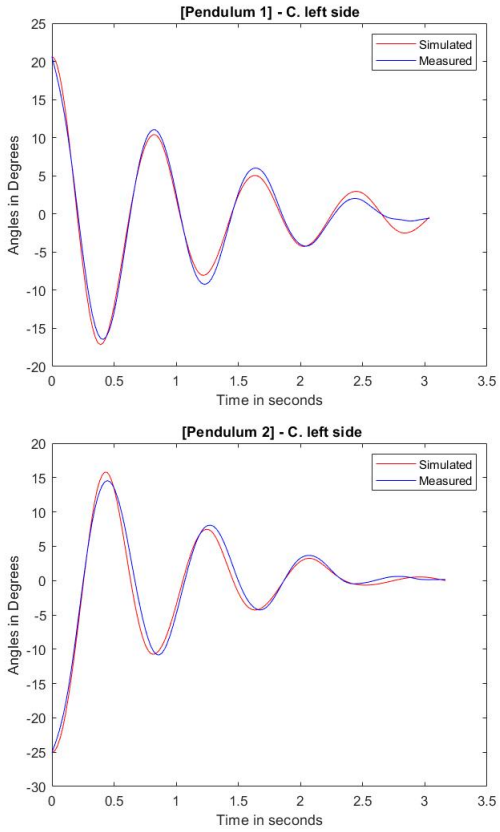

Fig. 6. Experimental **(measured)** and modeled **(simulated)** knee trajectory for the initial condition in extension (pendulum 1) and flexion (pendulum 2).

The values obtained for the final chromosome of each pendulum are presented in Table III. Values of those chromosomes are in the order of magnitude as the ones described in [6]. Those models will be used to be the reference to reach for the control part in the next section.

b) For C: For those models, velocity and position feedback torques are considered as C represents the spastic case. These results also highlight the same amplitudes and frequencies between the simulated and measured data. Figure 6 presents the comparison between experiment and model with $R^2 = 99.3\%$ (mean error: $0.09° \pm 0.85°$) for pendulum 1 and $R^2 = 98.2\%$ (mean error: $0.39° \pm 1.06°$) of for pendulum 2 .

The values obtained for the final chromosome presented in Table II of each pendulum were compared to the ones of the passive plant [6]. Velocity feedback gains obtained were also compared and are in the same range [6].

IV. Control of the spasticity using PID controller and GA

After the modeling of the knee's angular displacement of the twins, the next step is to control the knee angular trajectory of C by using a PID controller to converge towards the one of H. Management of spasticity does not directly include forcing the limbs into the spastic region but the goal of this controller is to determine what range the correction can reach. Indeed, a complete correction is the aim to achieve after several months or even years of rehabilitation.

A. Representation of the control

The interface between the exoskeleton and the lower limbs must be modeled for a better design of the exoskeleton and the motor specification. It is essential to determine how we are going to model the interface between the human (child) and the exoskeleton (only represented here as a simple motor) [27]. This connection is not unalterable. When assisting, the exoskeleton applied constraints on the soft tissues of the body. These tissues get deformed under the pressure applied by the device. The interface between the human and the exoskeleton is simply defined as a torsion torque $T_{torsion}$ with spring and damping contribution (Figure 7) [21].
All the different parts of this model are represented in Figure 8 and are determined further.

The torsion torque $T_{torsion}$ can be defined as :

$$T_{torsion} = S(\Theta_m - \Theta_k) + D(\Theta'_m - \Theta'_k) \qquad (4)$$

with:
S and D: gains respectively for the spring and the damper,
Θ_m, Θ_k: angular position of the motor and the human knee,

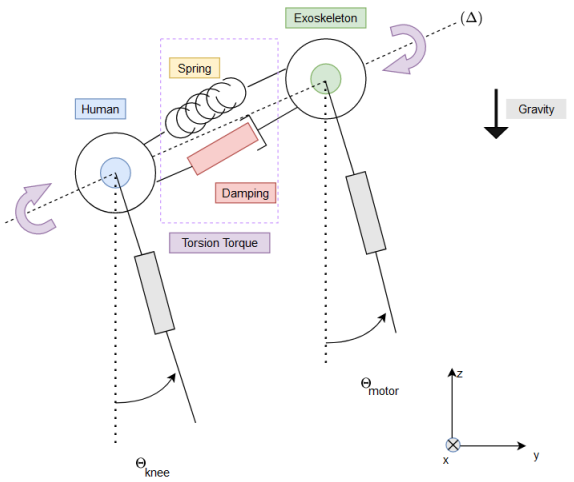

Fig. 7. Scheme of the torsion torque composed of a spring and a damper.

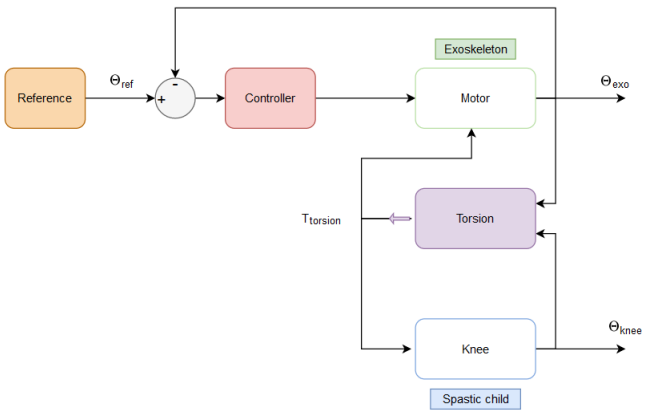

Fig. 8. Schematic view of the control with all the main systems: exoskeleton, human, interface and controller.

Θ'_m, Θ'_k: angular velocity of the motor and the human knee.

1) Spastic knee: For the spastic knee, the pendulum modeling of C. is used. Based on the equations seen in the *Methods* section (II.A), the torsion torque $T_{torsion}$ will be added as a help for the movement of the human to counteract the effect of the velocity-dependent torque which represents the spasticity. $T_{torsion}$ is instead seen as a brake for the exoskeleton which prevents it to perform the reference movement. Both cases are described in Equation 5.

$$I\Theta'' + B_{e,f}\Theta' + K_{e,f}\Theta + T_{e,f} + B\Theta' + K\Theta \pm T_{torsion} = mgLsin(\Theta) \quad (5)$$

The parameters in those equations are the same as those explained in the *Methods* section (II.A) and for the values, the chromosome determined in Table II is used.

2) Motor: For this model, an FLA-20A-09HP-H24 motor from Harmonic Drive with the parameters presented in Table V is chosen. Those motors are known to be used to power exoskeletons like in [28].

TABLE V
PARAMETERS OF THE FLA-20A-09HP-H24 MOTOR

Parameter	Value
Reduction	9
Inertia (kg.m^2)	0.0026
Ke (V.rad^{-1}.s^{-1})	0.56
Kc (N.m.A^{-1})	0.51
R (ohm)	0.03
L (mH)	0.07

Using the mechanical and electrical equations of the motor, a model is designed (Figure 9). The saturation boxes and the reduction are not represented in the following figure but are considered in the model. It will be considered as

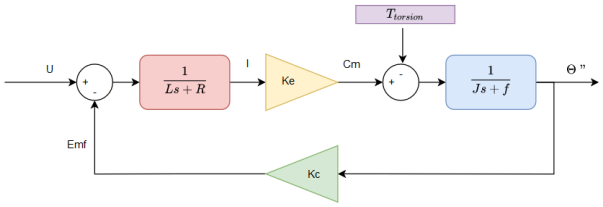

Fig. 9. Block diagram of the motor.

a restraint for the motor as we consider that the human will refrain from the movement of the motor. The friction coefficient f is set to 0.

3) PID controller: PID controller is a common method to correct errors (defined as the gap between the reference and the measure) and to control a system that can be a simple motor or a more complex system [29]. The controller

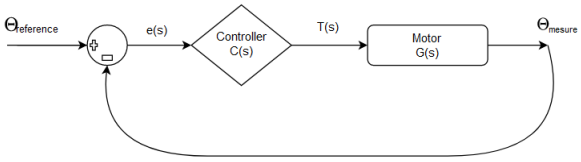

Fig. 10. Controller block diagram

C(s) represented in Figure 10 minimizes the error *e(s)* and products a torque *T(s)* applied to the plant studied (here, a motor *G(s)*). The error is then computed as the difference between the input ($\Theta_{reference}$) and the output of the motor (Θ_{exo}). The controller *C(s)* can be defined as follows:

$$C(s) = K_p + \frac{K_i}{s} + K_d s \quad (6)$$

Different ways exist to define the PID parameters (K_p, K_i, K_d) [30] as Ziegler-Nichols method (Z-N) [18] but also Genetic Algorithm (GA) and Particle Swarm Optimization Algorithm (PSO) [31]. GA and PSO are known to be used for optimization problems which is our case: the model must have the best parameters to optimize the knee trajectory control of the spastic child. In this paper, GA was chosen for determining those parameters.

4) Position reference: For the reference, the pendulum modeling of H. was chosen. The parameters of the model used are those presented in Table III. Thus, the angular position ($\Theta_{reference}$) is used to be the reference for the motor and to compute the error *e(s)*.

B. PID and torsion torque parameters using GA

The PID parameters (K_p, K_i, K_d) and the torsion torque parameters *(S, D)* remain unknown in our model. To determine them, GA was defined in the *Methods* part (II.A) as in [17],[7]. The chromosome to be determined by the GA for this part is defined as follows :

$$C = [S, D, K_p, K_i, K_d] \tag{7}$$

The genetic algorithm was computed with the following parameters:

- Number of parameters to determine: 5,
- Number of iterations: 10000,
- Number of chromosomes to test at each iteration: 3000,
- Maximum stall generation: 100,
- Function tolerance value: $1e^{-5}$.

To determine the best chromosome, the cost function used is the same as defined previously. The cost function is here based on the error between the angular reference position and the angular position of the spastic child's knee.

C. Results

TABLE VI
TORSION TORQUE AND PID CONTROLLER PARAMETERS FOR BOTH PENDULUM CONTROLS

Parameter	Pendulum 1	Pendulum 2
$S[N.m.rad^{-1}]$	8	8
$D[N.m.rad^{-1}.s^{-1}]$	2	2
K_p	99.88	86.2
K_i	302.88	161.4
K_d	-0.98	-0.5

To run the model, the same initial conditions (angular position and speed for extension or flexion) for the spastic model and the reference model were used.

a) For flexion as the initial condition: The pendulum 2 of H. and the pendulum 2 of C. are computed and presented in Figure 11.

The angular position of C. improved. The frequency converges to the one of H. and there is the same observation for the amplitude of the movement. $R^2 = 93\%$ (mean error: $0.06° \pm 2.18°$).

b) For extension as the initial condition: The pendulum 1 of H. and the pendulum 1 of C. are computed as presented in Figure 11.

As for the flexion, the angular position of C. improved. The frequency converged to the one of H. and there is also the same observation for the amplitude of the movement. $R^2 = 87\%$ (mean error: $-1.41° \pm 1.9°$).

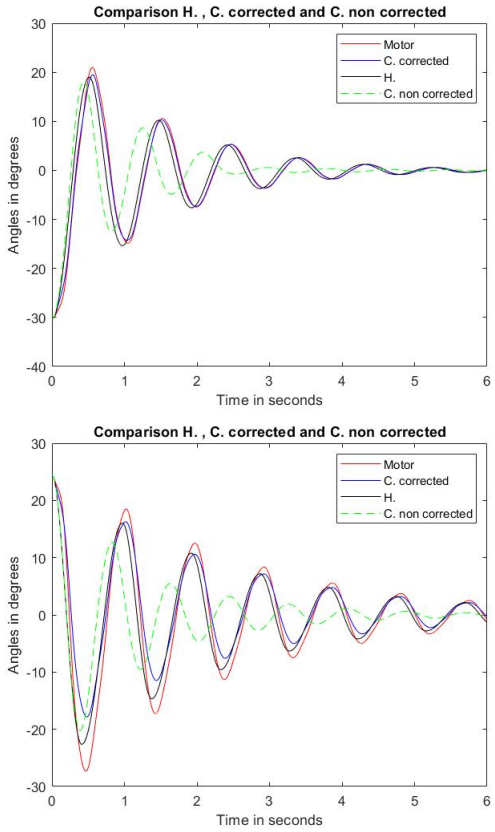

Fig. 11. Knee Angular position evolution of C. corrected (blue), C. non-corrected (green), H. (**black**) and motor angular position evolution (red), for flexion and extension initial conditions.

The results obtained for flexion and extension allow concluding that this method is accurate enough to correct the angular trajectory of C to fit the one of H. Rehabilitation of spastic subjects does not consider fully recovering the range of motion with short delays. Thus, those results are preliminary results to continue the investigation and modulation of the control. These results were obtained with the chromosome detailed in Table VI.

The same torsion torque was considered for both pendulums as it is supposed that the interface is the same in both cases. The integral gain is higher than the other one to allow the total correction of the static error. The proportional gain is also important to diminish the rise time. Damping and the stiffness coefficient are very important for the correction of the spastic angular trajectory. Variations of S and D can create different results and can conduct to the wrong behavior of the knee.

V. CONCLUSIONS AND DISCUSSIONS

The aim of this paper is to model and control the angular position of the knee of a child with spastic cerebral palsy. The main contribution and novelty of this paper is the personalised model of spasticity including position-dependent torques whose gains have been found using a method based on a GA. The interface between the timing of those torques and muscle activations was realized to support the major role

of spastic muscles in the spasticity model which was not stated in the literature. Finally, a damped elastic mechanical system was defined to model the interface between human and exoskeleton whose parameters were defined using GA. The modeling of the spasticity using data from EMG, velocity and position-dependent torques allowed to generate similar behaviour when compared to the experimental data from H. and C. Two initial conditions were tested (flexion and extension) which is not common in the literature. The R^2 results allow demonstration of the relevance of this method. Then, to correct the angular position of the spastic knee, a PID controller was set and a spring-damping torsion torque was defined between the knee and the exoskeleton. The parameters were optimized using GA and give accurate results quantified by the R^2 method.

This study was mainly focused and personalised for data of two twin sisters which are not representative of a huge population. Indeed, the project aims to realize a customized exoskeleton for each spastic subject. Other cases of study can be done with other twins or other children with spastic cerebral palsy. The same method will be used but different results are expected as the pathology varies greatly from one individual to another. Moreover, only the angular trajectory of the knee is studied here with a single degree of freedom which allows us to focus on designing the model. Indeed, spastic cerebral palsy has more effect on knee extension and flexion movements.

After the pendulum test, future works will focus on kinematic and dynamic data of different gaits of these two subjects and will target the correction of a walking gait. For this purpose, an entire exoskeleton will be modeled and controlled.

ACKNOWLEDGEMENT

The authors would like to thank the Région Occitanie and Université Fédérale Toulouse Midi-Pyrénées (UFTMIP) for their financial support.

CONFLICT OF INTEREST STATEMENT

The authors confirm that there are no conflicts of interest regarding the work described in the current manuscript.

REFERENCES

[1] P. Rosenbaum, "Cerebral palsy: what parents and doctors want to know," *BMJ (Clinical research ed.),*, vol. 326(7396), p. 970–974., 2003.

[2] H. K. Graham, "Pendulum test in cerebral palsy," *Lancet (London, England)*, vol. 355(9222), p. 2184, 2000.

[3] P. O. Pharoah, T. Cooke, I. Rosenbloom, and R. W. Cooke, "Trends in birth prevalence of cerebral palsy." *Archives of disease in childhood*, vol. 62(4), p. 379–384, 1987.

[4] J. W. Lance, "What is spasticity?" *Lancet (London, England)*, vol. 335(8689), pp. 108–115, 1990.

[5] A. Kheder and K. P. Nair, "Spasticity: pathophysiology, evaluation and management," *Practical neurology*, vol. 12(5), p. 289–298, 2012.

[6] J. Fee, J. W. and R. A. Foulds, "Neuromuscular modeling of spasticity in cerebral palsy," *IEEE transactions on neural systems and rehabilitation engineering : a publication of the IEEE Engineering in Medicine and Biology Society*, vol. 12(1), p. 55–64, 2004.

[7] M. R. Dimitrijevic, "Spasticity," *Scientific Basis of Clinical Neurology*, pp. 108–115, 1985.

[8] Y. N. Wu, H. S. Park, J. J. Chen, Y. Ren, and L. Q. Roth, E. J.and Zhang, "Position as well as velocity dependence of spasticity-four-dimensional characterizations of catch angle," *P. Frontiers in neurology*, vol. 9, 2018.

[9] T. Rekand, "Clinical assessment and management of spasticity: a review." *Acta Neurologica Scandinavica*, pp. 122: 62–66, 2010.

[10] R. Wartenberg, "Pendulousness of the legs as a diagnostic test," *Neurology*, vol. 1, no. 1, pp. 18–18, 1951. [Online]. Available: https://n.neurology.org/content/1/1/18

[11] T. Bajd and B. Bowman, "Testing and modeling of spasticity," *Journal of biomedical engineering*, vol. 4(2), pp. 90–96, 1982.

[12] . V. L. Bajd, T., "Pendulum testing of spasticity," *Journal of biomedical engineering*, vol. 6(1), pp. 9–16, 1984.

[13] T. Bajd and B. Bowman, "Testing and modelling of spasticity," *Journal of biomedical engineering*, vol. 4(2), pp. 90–96, 1982.

[14] P. Le Cavorzin, S. Poudens, F. Chagneau, G. Carrault, H. Allain, and P. Rochcongar, "A comprehensive model of spastic hypertonia derived from the pendulum test of the leg," *Muscle Nerve*, vol. 24, pp. 1612–1621, 2001.

[15] W. Yu and J. Rosen, "Neural pid control of robot manipulators with application to an upper limb exoskeleton," *IEEE transactions on systems, man, and cybernetics. Part B, Cybernetics : a publication of the IEEE Systems, Man, and Cybernetics Society*, vol. 43, 09 2012.

[16] Z. F. Lerner, D. L. Damiano, H.-S. Park, A. J. Gravunder, and T. C. Bulea, "A robotic exoskeleton for treatment of crouch gait in children with cerebral palsy: Design and initial application," *IEEE Transactions on Neural Systems and Rehabilitation Engineering*, vol. 25, no. 6, pp. 650–659, 2017.

[17] M. S. Amiri, R. Ramli, and M. F. Ibrahim, "Hybrid design of pid controller for four dof lower limb exoskeleton," *Applied Mathematical Modelling*, vol. 72, pp. 17–27, 2019.

[18] J. Ziegler and N. Nichols, "Optimum settings for automatic controllers," *Transactions of the ASME*, vol. 64, pp. 759–768, 1942.

[19] M. S. Amiri, R. B. Ramli, M. F. Ibrahim, D. A. Wahab, and N. K. Aliman, "Adaptive particle swarm optimization of pid gain tuning for lower-limb human exoskeleton in virtual environment," 2020.

[20] N. Jarrasse and G. Morel, "Connecting a human limb to an exoskeleton," *IEEE Transactions on Robotics*, vol. 28, pp. 697–710, 01 2011.

[21] Y. Huo, X. Li, X. Zhang, and D. Sun, "Intention-driven variable impedance control for physical human-robot interaction," in *2021 IEEE/ASME International Conference on Advanced Intelligent Mechatronics (AIM)*. IEEE, 2021, pp. 1220–1225.

[22] H. J. Hermens, B. Freriks, C. Disselhorst-Klug, and G. Rau, "Development of recommendations for semg sensors and sensor placement procedures. journal of electromyography and kinesiology," *International Society of Electrophysiological Kinesiology*, vol. 10(5), p. 361–374, 2000.

[23] R. K. Jensen, "Body segment mass, radius and radius of gyration proportions of children," *Journal of biomechanics*, vol. 19(5), p. 359–368, 1986.

[24] J. Winters, "Generalized analysis and design of antagonistic muscle models: Effect of nonlinear muscle properties on the control of fundamental movements," *Ph.D. dissertation, Univ. Calif., Berkeley, CA*, 1985.

[25] J. H. Holland, *Adaptation in natural and artificial systems: an introductory analysis with applications to biology, control, and artificial intelligence*. MIT press, 1992.

[26] D. Winter, "The biomechanics and motor control of human gait." *University of Waterloo Press, Waterloo, Ontario*, 1987.

[27] N. Jarrasse and G. Morel, "Connecting a human limb to an exoskeleton," *IEEE Transactions on Robotics*, vol. 28 (3), pp. 697–709, 2012.

[28] H. Aguilar-Sierra, W. Yu, S. Salazar, and R. López, "Design and control of hybrid actuation lower limb exoskeleton," *Advance in Mechanical Engineering*, vol. 7, 2015.

[29] G. C. Kiam Heong Ang and Y. Li, "Pid control system analysis, design, and technology," *IEEE Transactions on Control Systems Technology*, vol. 13, no. 4, pp. 559–576, 2005.

[30] M. A. Unar, D. J. Murray-Smith, and S. F. A. Shah, "Design and tuning of fixed structure pid controllers- a survey [research report]," University of Glasgow, Glasgow, Scotland, UK., Tech. Rep., 1995.

[31] I. Muhammad, H. Rathiah, and N. E. Abd Khalid, "An overview of particle swarm optimisation variants," *Procedia Engineering*, vol. 53, pp. 491–496, 2013.